5-2022

Using Deep Learning with Satellite Imagery to Estimate Deforestation Rates

Maeve Naughton-Rockwell
William & Mary

WILLIAM & MARY
CHARTERED 1693

THE COLLEGE OF WILLIAM & MARY

HONORS THESIS

Using Deep Learning with Satellite Imagery to Estimate Global Deforestation Rates

---

Author:
Maeve
NAUGHTON-ROCKWELL

Advisor:
Dan RUNFOLA

A thesis submitted in fulfillment of the requirements for Interdisciplinary Honors in the degree of Bachelors of Science in the

Data Science Program

Accepted for Honors

Chair: Dr. Dan Runfola

Dr. Robert Rose

Dr. Anthony Stefanidis

Williamsburg, Virginia May 4, 2020

THE COLLEGE OF WILLIAM & MARY

Abstract

Dr. Dan Runfola
Data Science Program

Bachelors of Science

Using Deep Learning with Satellite Imagery to Estimate Global Deforestation Rates

by Maeve NAUGHTON-ROCKWELL

Previous studies have used Convolutional Neural Networks for regional detection of deforestation breaks. However, there is limited research into the capability of deep neural networks to identify sudden shifts in global forest cover from satellite imagery. Additionally, many deforestation detection models are trained on region specific data and need manual input thresholds. In this work, we develop a deep learning model to predict the percent of deforestation in a region between two points in time, trained on globally sourced data. Using the before and after satellite images of a deforestation event as inputs, we implemented a two input Convolutional Neural Network with ResNet transfer learning. The model yields a percent estimate of the deforestation that occurred within the region, achieving an error of 7.61%, using thousands of observations across a wide range of bio-climatic regions. These results illustrate the ability of a deep learning model to predict deforestation when it occurs, at a global scale. Our study, which uses random sampling from every continent, suggests the efficacy/possibility of moving from a limited and regional method to a global model.

Contents

List of Figures

List of Tables

List of Abbreviations

FAO	Food & Agriculture Organization
CNN	Convolutional Neural Network
RGB	Red, Green, and Blue
TOA	Top of Atmosphere
USGS	United States Geological Survey
NDVI	Normalized Difference Vegetation Index
BFAST	Breaks for Added Season and Trend
MAE	Mean Absolute Error
MAPE	Mean Absolute Percent Error

Chapter 1

Thesis

1 Introduction

With rising concern for climate change and unprecedented deforestation rates in the Brazilian Amazon, it is increasingly important to create effective deforestation detection methods (Shyamsundar et al., 2021; Zon and Sparhawk, 1923). Though the research community has focused heavily on deforestation detection, there are significant gaps in the capabilities of contemporary methods. Specifically, most current methods of deforestation detection are region specific and often require manual threshold inputs (Buhalău, 2016; Schroeder et al., 2011; Banskota et al., 2014).

In this work, we explore the capability of deep learning techniques to identify the degree of deforestation in satellite images captured at any two points in time. We specifically focus on the efficacy of a single model to capture these trends globally, irrespective of shifts in bioclimatic regime. This paper seeks to answer the research question: *To what degree can deforestation be quantified using deep learning techniques?*

To explore this question, we leverage global Landsat satellite imagery and train a neural network to predict the percent of deforestation that occurred in a region. We define forest cover as a 30mx30m pixel that has at least 25% canopy closure of trees over 5m tall (Hansen, Stehman, and Potapov, 2010) and deforestation as forest cover that is removed due to any type of disturbance (Hansen, Stehman, and Potapov, 2010).

This paper is structured as follows. In section 2, we provide a literature review comparing past deforestation detection models. In section 3, we explain how we acquired and processed the deforestation data and satellite imagery

inputs. Section 4 and 5 detail the methods for the model architecture created, followed by the results. Sections 6 and 7 provide our discussion and a brief conclusion.

2 Literature Review

Forests play an important role in shaping local and global ecosystems, covering 31 percent of the global land area (Schroeder et al., 2011; Banskota et al., 2014; FAO, 2020). Forests are important and unique habitats for animals, providing 4.06 billion hectares of unique terrain (FAO, 2020). Trees have numerous ecological benefits for ecosystems, economic benefits to humans, and play a large part in regulating the climate (Miura et al., 2015). Forests also contribute to the livelihoods of subsistence farmers and provide a major energy source in many developing countries (FAO, 2015; FAO, 2020; Romijn et al., 2015; Boafo, 2013). However, forests are a limited resource, declining in size. It is estimated that since 1990 the Earth has lost 420 million hectares of forest with agricultural expansion being the primary cause (FAO, 2020).

The destruction of forests can have negative environmental and ecological effects, especially on tropical countries (D'Almeida et al., 2007; Amelung, 1993). Deforestation can change the microclimate, influence soil erosion, and decrease habitat for animals in these areas (Viera et al., 2008). The unique ecology of rainforests lends itself to the adaptation of rare species of flora and fauna only found in uncommon conditions (Amelung, 1993; Klaus Riede, 1993). The loss of this particular habitat irreversibly threatens the biodiversity of species, allowing for their endangerment (Viera et al., 2008).

Increasing variability in weather can decrease tourism and can be an economic damper as many cities depend on eco-tourism (Amelung, 1993). These changing environmental factors can also decrease agricultural productivity in tropical areas (Amelung, 1993). Deforestation also has the ability to greatly increase global greenhouse gasses (Galford et al., 2010). Trees sequester carbon and the release of this carbon affects the climate (Cramer, Bondeau, and Schaphoff, 2004; Foley et al., 2005, Romijn et al., 2015). It is estimated that forests

contain around 80 percent of the total carbon in the terrestrial above ground biosphere (Waring and Running, 1998). The release of sequestered carbon from deforestation can have substantial effects on the amount of greenhouse gasses in the atmosphere (Galford et al., 2010).

Alongside the need to protect forests, there is an immediate urgency to keep accurate records for forest monitoring programs such as REDD and REDD+ (UN-REDD, 2014). However, global forest data has not always been available. It was not until 1923, when the first Global Forest Resource Assessment was published, that we had any idea of the volume of forests on Earth (Zon and Sparhawk, 1923). Since 1948, the United Nations's Food and Agriculture Organization (FAO) has performed forest assessments every five to ten years (MacDicken, 2015). In recent years, great strides have been made in tracking forest loss with satellite imagery (Hansen et al., 2013;Finer et al., 2018; Belward and Skøien, 2015). A popular satellite which has led to the development of many deforestation monitoring programs is the USGS Landsat series (Lechler et al., 2020; Hansen et al., 2013; Hansen, Stehman, and Potapov, 2010). The first Landsat satellite was launched by USGS in 1972 and the program has since launched 8 successful satellites, providing continuous Earth data for over 40 years (Roy et al., 2014). Our ability to monitor forests continues to develop and improve as our remote sensing capabilities increase. From 2005 to 2015 the total tropical forest area monitored increased from 69% to 83% (Romijn et al., 2015). The increasing availability of free and open remote sensing data has greatly expanded the scope of what land can be monitored (Romijn et al., 2015).

2.1 Contemporary Approaches to Measure Breaks in Forests

Satellite observations of forest cover have become the primary approach for the measurement of forest health and size, with 70% of global forest assessments using such imagery as recently as 2015 (MacDicken, 2015). The long history, accessibility, and reliability of the Landsat series of satellites has been one of the most important contributors to this use, providing nearly 40 years of unbroken coverage of land cover at comparable temporal, spectral, and radiometric resolutions (Lauer, 1997). While many contemporary satellites have higher resolutions, this long-term record has improved our capability to understand the evolution of

forest cover throughout much of contemporary human history (Keenan et al., 2015).

One major challenge to the use of satellite data to monitor forest cover is how to translate the spectral signatures observed (generally across visual and near-infrared bands) into estimates of forest cover, or the quantity of other vegetative biomass present on the earth's surface (Schroeder et al., 2011). The manipulation of image bands is one way to reformat images to isolate a study object, with many different ways to highlight vegetation (Banskota et al., 2014). A common method is highlighting green vegetation by manipulating the red and Near-Infrared (NIR) bands to create a Normalized Difference Vegetation Index (NDVI) (Eckert et al., 2015, Nath and Acharjee, 2013). The NDVI maximizes the contrast between greenness and spectral background and can be used to create phenological profiles for specific forest regions. In 2018, Othman et al. performed an assessment of Malaysian tropical forest vegetation cover using NDVI on 1km and 250m resolution MODIS images (Othman et al., 2018). For the 250m resolution images Othman found that 8.9% of the total forest was degraded with a 70-90% accuracy. The study suggested that imagery with higher resolution had more accurate results.

Some studies have found that NDVI does not always have the accuracy that is promised (Schroeder et al., 2011). In 2011 Schroeder et al. performed a comparison study of various band calculations and indices using Landsat Time Series annual image composites to determine when and what type of disturbance to the forest occurred (Schroeder et al., 2011). Schroeder tested Short-Wave Infrared (SWIR), Tasseled Cap Wetness, Forestness Index, NDVI, normalized burn ratio (NBR), Tasseled Cap angle, and other green leaf indices. This study found that the SWIR band was the most effective in differentiating between fires and clearcut harvests, even up to 4 years after the disturbance occurred. Schroeder found that NDVI and other near infrared-based indices led to lower classification accuracy. To accommodate for this, researchers have developed numerous variations of NDVI in attempt to cover its weaknesses: Soil Adjusted Vegetation Index (SAVI), Enhanced Vegetation Index (EVI), and Atmospheric Resistant Vegetation Index (ARVI) (Huete, 1988;Jiang et al., 2008;Kaufman and Tanre, 1992).

One weakness of vegetation detection algorithms is that they do not inherently identify when deforestation occurs (Verbesselt et al., 2010a). Breaks for Additive Season and Trend (BFAST) is a change detection method that uses a time-series to identify a stable historical period to compare breaks against (Verbesselt, Zeileis, and Herold, 2012; Hamunyela et al., 2020). BFAST integrates the decomposition of time series into trend, seasonal, and remainder components with methods to detect breaks (Verbesselt et al., 2010a). BFAST can provide near-real time deforestation detection and can identify breaks in long-term seasonal patterns using RGB imagery or a vegetation index (Verbesselt et al., 2010a;Gao et al., 2021).

BFAST has been proven to be a useful tool to identify deforestation events using satellite imagery and remote sensing indices. The BFAST time-series change-detection algorithm identifies pixels that deviate significantly as breakpoints (Mitchell, Rosenqvist, and Mora, 2017;Verbesselt et al., 2010a). BFAST iteratively estimates the time and number of changes based on a magnitude threshold (Verbesselt et al., 2010a). In 2016, Bahalau found that using BFAST with Normalized Difference Moisture Index (NDMI) had greater accuracy than BFAST using NDVI (Buhalău, 2016). In 2018 Schultz found that using BFASTmonitor with NDMI performed best with closed canopies versus open canopies (Schultz et al., 2018). Lechler et al. compared multiple types of forest health indices with BFAST and Random Forest algorithm, finding that SAVI used as input for BFAST has the highest accuracy (Lechler et al., 2020).

Another threshold-based change detection method used is the Vegetation Change Tracker (VCT) which uses the Integrated Forest z-score (IFZ) as a spectral variable in time-series analysis (Banskota et al., 2014; Huang et al., 2010). VCT works by first masking each image from clouds, water, and cloud shadow using low reflectance values and NDVI. Then a band calculation is performed that determines the likelihood of each pixel representing forest by calculating the IFZ. From this index a final change and no change class layer is created; however, it only achieved accuracy of 80% (Huang et al., 2010). The downside of using a threshold based technique is that it is region specific and empirically determined. A threshold that is calculated for one area is not interchangeable with other regions containing different vegetation types and densities (Banskota et al., 2014).

2.2 Deep Learning with Satellite Imagery

The sheer amount of remote sensing data that is available has led to developments in creating deep learning models with satellite imagery. For example, deep learning models have been shown to outperform traditional remote sensing techniques in the context of segmentation (Minaee et al., 2020), scene classification (Alhindi et al., 2018), and even land cover change detection (Sefrin, Riese, and Keller, 2021). However, there is limited literature on using Deep Learning to detect forest disturbances (Kislov et al., 2021).

A CNN is a deep learning model that uses sequential filters to identify patterns and structures (Sylvain, Drolet, and Brown, 2019). CNNs are made up of layers with interconnected nodes that receive and pass on weights (Minaee et al., 2020). In 2021 Kislov et al. used pansharped, high resolution satellite imagery with a deep convolutional neural network (DCNNs) to determine forest damage caused by certain pests (Kislov et al., 2021). Kislov used an encoder-decoder network architecture with U-Net. It was found that DCNNs performed better than traditional pixel-based classification methods (Kislov et al., 2021).

In 2019 a study was performed using high-resolution (<5m) classifying satellite imagery as either forest or not forest using three popular CNN structures: ResNet, DenseNet, and U-Net. It was found that U-Net performed best with an accuracy of 88.27% and an F1-score of 86.29%. (Mazza et al., 2019). U-Net has been used in various deep learning studies on high resolution forest satellite imagery. In a study on wind-related deforestation detection, U-Net was further extended with an additional dropout layer and batch normalization after each convolutional layer that could be parameterized at each step. This created a U-Net-like CNN that achieved up to 97% accuracy at determining wind damaged sites in certain forested landscapes. This study found that a U-Net-like CNN is better at handling pattern-specific sources of error compared to pixel-based methods (Kislov and Korznikov, 2020; Kislov et al., 2021).

Studies employing traditional CNN architectures tend to exhibit similar levels of accuracy to those employing more complex U-Net approaches. In one study on road segmentation it was found that Fully Connected Neural Networks (FCN) perform 1.5% better on inputs of 512 x 512 pixels and U-Net performs 6% better on inputs of 256 x 256 pixels. However, it was found that U-Net overfit the data for both input sizes while the FCN had either an equivalent or

higher validation accuracy to training accuracy (Ozturk, Saritürk, and Seker, 2020). Because of the class imbalance of the forested and deforested pixels in the Landsat data used in this study, it is important to watch for overfitting. Studies have shown that U-Net performs poorly for detecting non-standard objects of interest, especially with changing terrain (Shahedi et al., 2020;Kislov et al., 2021).

Lobo Torres et al. tested six different neural network architectures on Landsat and Sentinel data for the purpose of deforestation detection in the Amazon (Torres et al., 2021). Lobo Torres et al. attempted to identify the pixels where deforestation occurred at the time interval between two co-registered images. Because the datasets were imbalanced with less than 1% of the data belonging to the deforestation class, they used a Weighted Cross-Entropy Loss. The models performed similarly on the Landsat and Sentinel data with a slight reduction in classification errors when using the Sentinel data. Overall, ResU-Net and FC-DenseNet were found to be the best performing. The ResU-Net is similar to the U-Net but has stacked layers of residual blocks to stop exploding or vanishing gradients. The FC-DenseNet is a Densely Connected Convolutional Network with added upsampling for the purpose of image classification (Torres et al., 2021).

A difficulty of creating a model detecting deforestation is finding accurate validation data. A popular dataset used is the Hansen et al. 2013 derived Global Forest Watch data (Hansen et al., 2013). This dataset contains several variables of note: Tree canopy cover for year 2000, Global forest cover loss 2000-2017 (Loss), Global forest cover gain 2000-2017 (Gain). Tree cover is defined as 25% canopy closure per pixel for all vegetation 5m and taller. Forest gain is defined as non-forest to forest change entirely within the study period. Forest loss is defined as change from a forest to non-forest state (Hansen et al., 2013).

In 2020 Galiatsatos performed an accuracy assessment on the Global Forest Change data using the Guyana-Measurement Reporting and Verification (MRV) and Landsat imagery (Galiatsatos et al., 2020). For this analysis, each pixel of Landsat imagery was labeled based on the estimated tree cover percentage. Tree cover was defined as a pixel where percent tree canopy coverage was at least 50%. It was found that the accuracy for forest loss when comparing the Global

Forest Change dataset and Guyana-MRV was around 99%. This study suggests that Global Forest Change data is more accurate than previously thought. Hansen et al. reported an accuracy of 80% or better in tropical biomes, while Galiastatos et al. found an accuracy of 99%.

Mitchard et al. 2015 also performed a study to determine the accuracy of the Hansen Forest Loss Data (Mitchard et al., 2015). Mitchard et al. looked at the usefulness of University of Maryland (UMD) Global Forest Change data for the UK's International Climate Finance (ICF) using two case studies in Brazil and Ghana. The satellite imagery used was 5m RapidEye and SPOT data. The Brazil imagery was put through a Support Vector Machine and the Ghana data went through a two layer neural network for classification. It was found that the Global Forest Watch dataset performed well in Brazil with an accuracy of 95% and relatively low errors of omission. The UMD dataset did not provide the same results for Ghana. In Ghana the UMD dataset only captured 10% of the deforestation. Deforestation in Ghana is typically driven by small agroforestry (Acheampong et al., 2019) and the 30m Landsat pixels were not able to capture the change in forest (Mitchard et al., 2015).

There is some debate on what the best spatial resolution to use for Deep Learning forest classifications is. A drawback of high resolution data is that it can be hard to find or expensive to produce and often not viable for larger study areas (Sefrin, Riese, and Keller, 2021). Kattenborn argues that the traditional method of pooling and convolving to lower spatial resolutions is not effective for vegetation mapping (Kattenborn, Eichel, and Fassnacht, 2019). Course spatial resolution can lead to errors of where exactly the deforestation occurred (Lunetta, 1991; Lepš and Hadincová, 1992;Leitão et al., 2018).

Much of the research on deforestation detection are small case studies and region specific.The imagery used to train the models concentrate on a specific continent or section of a country. There has not been much research on applications of deep learning to identify deforestation at a global scale. Some studies have found spatial bias from global models, with different accuracies per continent (Masolele et al., 2021). While other studies use satellite imagery with coarse spatial resolution (>250m) (Hansen, Stehman, and Potapov, 2010; Loveland et al., 2000; Hansen et al., 2013). The following sections of the paper attempt to address the gaps in global deforestation detection methods.

3 Data

3.1 Study Area

All regions that were measured by Hansen et al. 2013 (Hansen et al., 2013) were eligible for inclusion in this study, covering the vast majority of tropical regions around the globe (see Figure 1.1). This resulted in an eligible area of 238 10x10 degree tiles. From this set, a random sampling strategy was employed in which 21,750 sites were chosen, totaling to 152,250 km^2. The resulting final dataset encompasses a wide range of geographies (i.e., forest, urban, deserts, and fields) (see Figure 1.5).

3.2 Deforestation Validation Data

FIGURE 1.1: Example of the Forest Loss layer of the UMD Global Forest Change Dataset (Hansen et al., 2013)

This study uses the University of Maryland (UMD) Global Forest Change Dataset to create the deforestation validation data (Hansen et al., 2013). The Global Forest Change data is derived from Landsat data (30 meter spatial resolution) and has layers characterizing forest extent, loss, and gain from 2000-2019. Forest loss is defined as the area of forest cover removed due to any type of disturbance (Hansen, Stehman, and Potapov, 2010. Only the Forest Loss Year layer was used for this study. This data can be downloaded as 10x10 degree raster tiles which span the entire world; (noting only terrestrial regions were incorporated into this study). Each raster cell contains a value from 0 to 19, with 0 representing no deforestation detected and 1-19 representing the year of deforestation (2001-2019).

Once the raster tiles were downloaded, 21,750 points of deforestation were randomly selected. A 7km x 7km bounding box was drawn around each of the random points and the percent area of deforestation versus no deforestation was calculated. Percent deforestation was calculated by counting the number of pixels where deforestation was found, divided by the total number of pixels in the region. This percent of deforestation per 7km bounding box was used as the final prediction output for the model.

3.3 Landsat Imagery

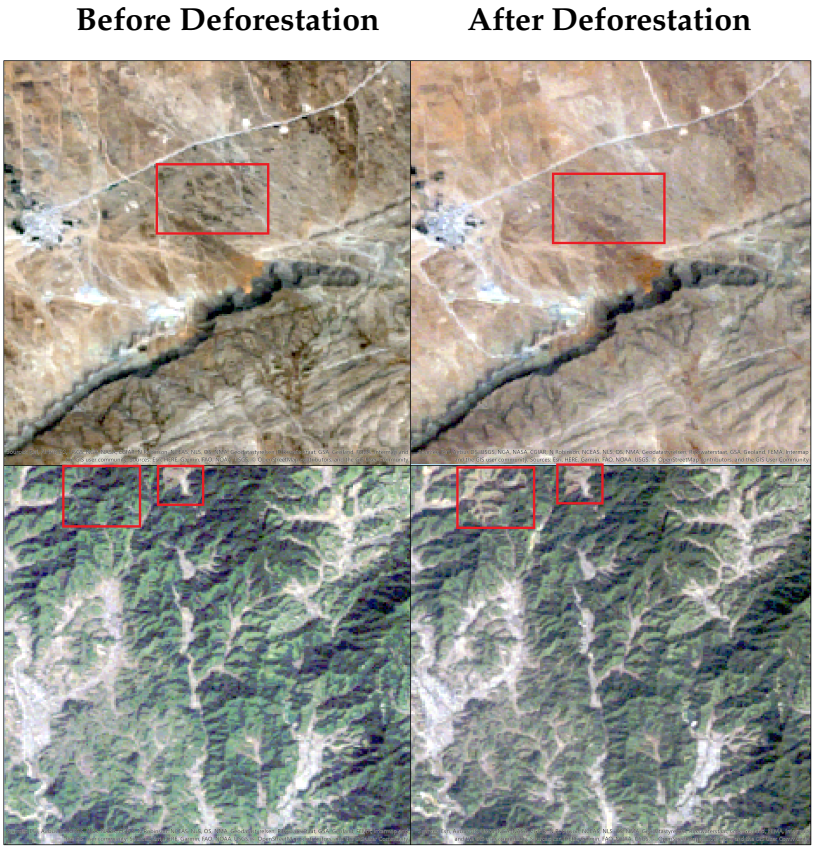

FIGURE 1.2: Example of Landsat imagery . Source image courtesy of the U.S. Geological Survey.

The USGS and NASA joint Landsat program has continuously collected satellite imagery since 1972 and put a total of 8 satellites in orbit. The Landsat 5 Thematic Mapper (TM) has 7 bands and operated from the years 1992 to 2013

(Chander, Markham, and Barsi, 2007). The Landsat 8 Operational Land Imager (OLI) has 9 bands and has operated since 2013 (Roy et al., 2014). Each satellite orbits around Earth every 99 minutes with a 16-day repeat cycle.

The satellite images used in this study were extracted from Landsat satellite 5 and 8 Tier 1 Collection 1 Top of Atmosphere (TOA) Reflectance (Woodcock et al., 2008). Tier 1 Collection 1 is the highest quality of data for Landsat, which has a radial root mean square error (RMSE) of 12 meters or less (USGS, 2018). Each pixel of a Landsat satellite represents 30 square meters.

Due to the ease of access and history of success the Global Forest Change data has with the Landsat satellites, Landsat 5 and 8 were used to collect the imagery for the study areas. We used the latitude and longitude of deforestation points derived from the Global Forest Change data as centroids for image download.

We downloaded one year composite images for the year before and the year after the identified deforestation date. For example, if deforestation was found in the year 2005, satellite imagery for the years 2004 and 2006 were downloaded. The images were sorted based on cloud coverage, and the least cloudy image for each year was chosen. The images were then clipped to a 7km bounding box and downloaded as red, green, and blue band files. As a final step for the image processing the band files were concatenated and transformed into PNG image files. The data was grouped into pairs with each pair containing the before and after image of a deforestation event of a single coordinate.

4 Methods

In our model, the outcome we are seeking to predict is the total deforestation between time 1 (a pre-deforestation scene, as measured by Hansen) and time 2 (a post-deforestation scene). We do this based on the pre- and post-imagery alone, leveraging a convolutional model. In this paper we develop two separate neural networks: a before neural network and an after neural network. The "before" neural network is given satellite images of a 7km region which depicts an area before a deforestation event occurs. The "after" neural network takes inputs of images after a deforestation event. The outputs of the two "before" and "after" CNNs are then concatenated and trained through a final series of

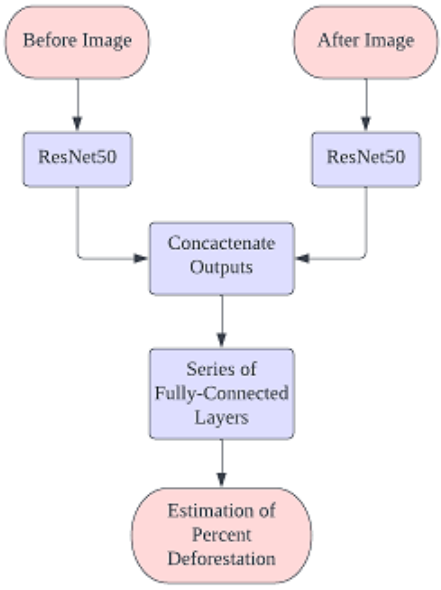

FIGURE 1.3: Flowchart of the Model used in paper

Fully-Connected Layers. The CNN created for this project was implemented using Tensorflow, an open source python package.

4.1 Train and Test Split

The 21,750 pairs of images were randomly separated into a 60/40 training and testing split. The training data set received 60% of the data, and the remaining 40% went into a testing dataset. Inside the training and testing datasets, the data was further divided. The grouped pairs of images were separated chronologically: with the earlier year belonging to the "before" dataset, and the more recent year placed into the "after" dataset.

4.2 Model Architecture

The model developed for this paper is a two step model that starts with two identical CNNs that feed into a final series of Fully-Connected Layers. For a single location, the before and after image of a deforestation event (size of 224 x 224) are fed into separate CNNs that are pretrained using transfer learning (based on the imagenet dataset (He et al., 2015)). Using the weights learned

from the classification of the ImageNet data, our model was fine tuned on the Landsat satellite imagery. The output from the ResNet50 model was then put through a series of dense layers.

Next, the "before" and "after" CNNs were concatenated and trained on a final network made of fully-connected dense layers using a Rectified Linear Unit (ReLU) activation function. We compiled the model using a batch size of 64, Adam optimization, and a learning rate of 0.0001. The optimization and learning rate were both chosen from a grid search. We then fine-tune the network parameterization over 50 epochs to estimate the percent deforestation of the $7km$ area.

5 Results

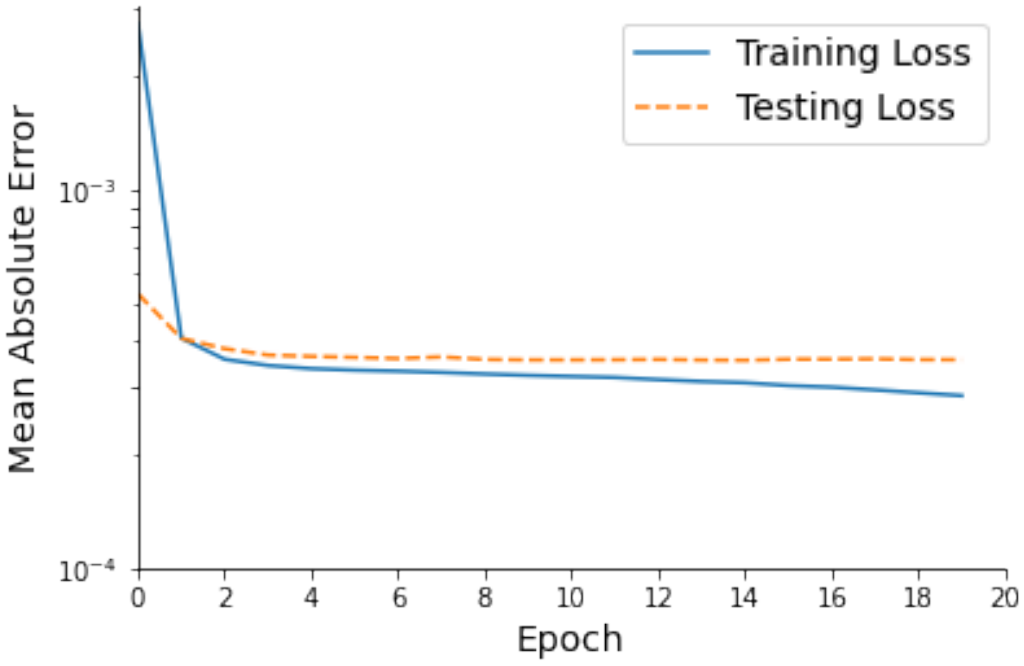

FIGURE 1.4: Graph of the MAE of the testing data every run of the epoch

Our CNN predicts the percent of deforestation that occurred in a 7km x 7km region with 7.61% error on a dataset of 21,750 locations. As indicated in Table

1.1, the average error per continent ranged from 4.79% (Europe) to 8.70% (South America). This model achieved an error of less than 10% for 85% of the testing dataset.

5.1 Results: Loss

Continent	MAPE	Number of Observations	Number of Outliers
Africa	5.15	1008	119
Asia	6.427	2659	497
Europe	4.79	775	74
N. America	7.45	1596	225
S. America	8.70	794	97
Australia	6.65	176	37

TABLE 1.1: Table for the error metrics of the testing data

Each epoch of the model was trained using the loss metric Mean Absolute Error (MAE). MAE, calculated as the average between the actual and predicted values, was chosen because of its resilience to outliers. Figure 1.4 depicts a sharp decrease in loss at the beginning of fitting and a steady decline in the loss each epoch. The final validation MAE of the model was 0.0003563 (i.e., 7.61% relative to the mean of 0.00468).

We report and evaluate the accuracy of the model using Mean Absolute Percent Error (MAPE), calculated as $MAPE = \frac{1}{n}\sum_{t=1}^{n}|\frac{A_t - P_t}{A_t}|$ where A is the actual percent of deforestation and P is the predicted percent of deforestation. The average percent deforestation for each input was 0.000468. Because the target values for this study are so small, even minute differences between the actual and predicted values result in large error. MAPE helps to account for this by showing inaccuracies as a percent of the target value.

5.2 Spatial Pattern of Errors

Figure 1.5 shows the percent error for each point of deforestation, mapped to the location of the event. This shows the breadth of samples from the study,

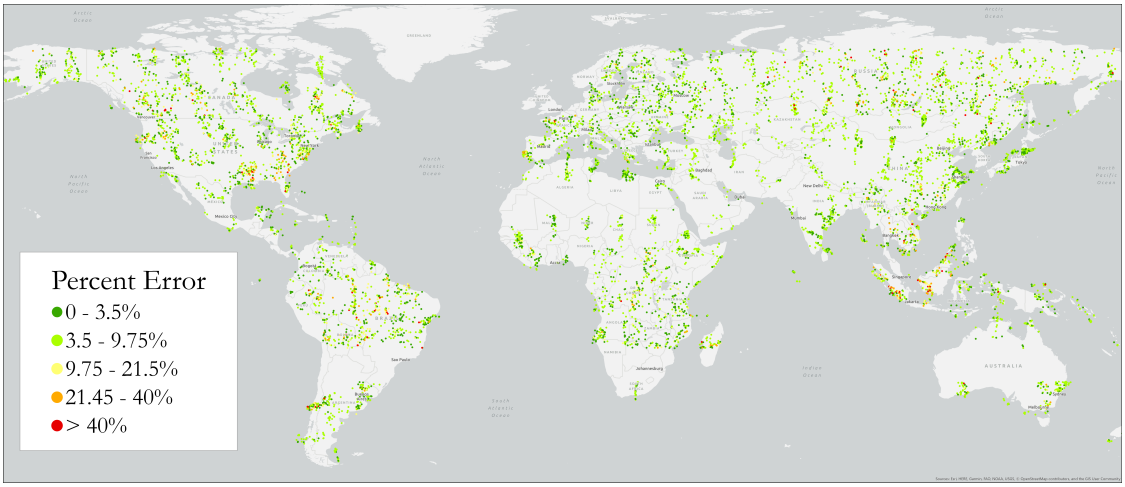

FIGURE 1.5: Map of the percent absolute error for each data point in the the testing dataset

Continent	Mean Percent Error (%)
Africa	5.14%
Asia	6.28%
Europe	4.79%
N. America	7.45%
S. America	8.70%
Australia	6.65%

TABLE 1.2: Mean Percent Absolute Error calculated from the testing dataset for each continent

with points across many different types of terrain in all continents. There do not appear to be large clusters of high errors.

In Figure A.4 we can see the percent error for each sample site in the testing dataset for Europe. The model achieved the lowest error in Europe. Though there are some points that resulted in above 40% error, Figure A.4 shows the even distribution of higher error points little appearance of clustering. This can be compared to the distributions of error in South America (see Figure A.6). South America has the highest percent error of the continents, however, the higher errors appear to be spread evenly across the land. There does not appear to be groups of high error in South America.

As you can see in Asia (see Figure A.3), the randomized sampling of deforestation led to diverse geographies in the training and testing datasets with

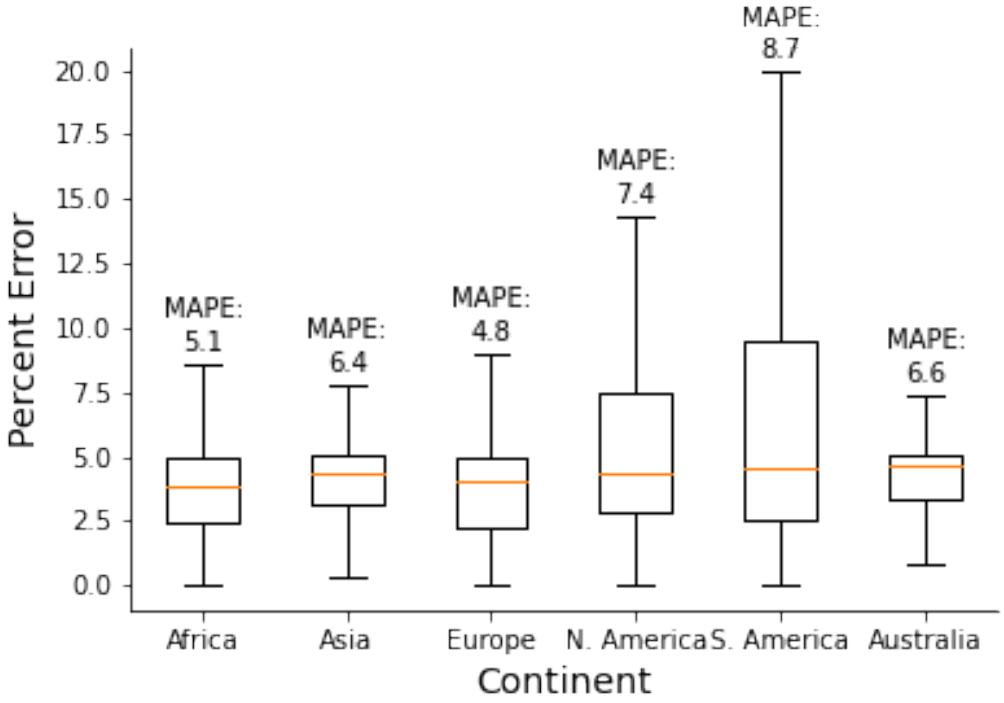

FIGURE 1.6: Relationship between percent error of the model and the continent the data point is found.

locations in mountains, deserts, islands, and more. In Asia there appear to be slight patterns in the error across the continent. There are occurrences of higher error in northern Asia and Oceania. We can also see slight groupings of error in North America (see Figure A.5). In North America the Central Canada and the South East region of the United States of America experience higher percent error.

In Australia Figure A.2 shows little grouping of high error, however, Australia has much lower sample size than other countries. The dataset has 176 observations from Australia compared to 2,659 observations inside Asia. Though Australia has the smallest interquartile range (Figure 1.6), it has the third largest MAPE. South America has the widest interquartile range and highest error.

When studying such a large area, it is important to break the data by region to evaluate any bias in error. For this study we examined the data by continent to determine if there were any spatial patterns of error. Figure 1.6 shows the

Biosphere	Mean Percent Error	# of Observations
Boreal Forests/Taiga	6.87%	1,318
Deserts & Xeric Shrublands	4.40%	713
Flooded Grasslands & Savannas	7.58%	55
Mangroves	6.80%	16
Mediterranean Forests, Woodlands & Scrub	6.35%	194
Montane Grasslands & Shrublands	5.83%	236
Temperate Broadleaf & Mixed Forests	5.71%	1,075
Temperate Conifer Forests	8.97%	314
Temperate Grasslands, Savannas & Shrubs	7.14%	747
Tropical & Subtrop. Coniferous Forests	4.69%	20
Tropical & Subtrop. Dry Broadleaf Forests	6.90%	220
Trop. & Subtrop. Grasslands, Savannas & Shrubs	5.68%	707
Tropical & Subtrop. Moist Broadleaf Forests	8.83%	898
Tundra	6.07%	498

TABLE 1.3: Mean Percent Absolute Error calculated from the testing dataset for each continent

error distribution of the continents studied: Africa, Asia, Europe, North America, South America, and Australia. This figure further shows the skew of the error towards smaller percent loss. As referenced in 1.2, Europe has the smallest MAPE with a value of 4.79% and South America has the largest MAPE of 8.70%. This suggests that the CNN is useful across a wide range of geographic data.

Phenological differences in terrestrial biospheres can cause large differences in satellite imagery which makes it hard to differentiate between seasonal change and deforestation (Verbesselt et al., 2010a). These visual differences can pose a challenge for the model to learn (Verbesselt et al., 2010b). For example, in a deciduous forest, an image taken during leaf-off season could appear as deforestation when none has occurred. By examining error trends in different biospheres we can evaluate the model's capacity for handling seasonal change/different forests/diverse terrain/different types of forests.

To further evaluate the extent of geographic bias, we looked at the percent error of each biosphere. We used the dataset created by Ecoregion (Dinerstein et al., 2017) which divides and groups all terrestrial land into 15 biospheres. Using this data we grouped the testing validation data based on the biosphere

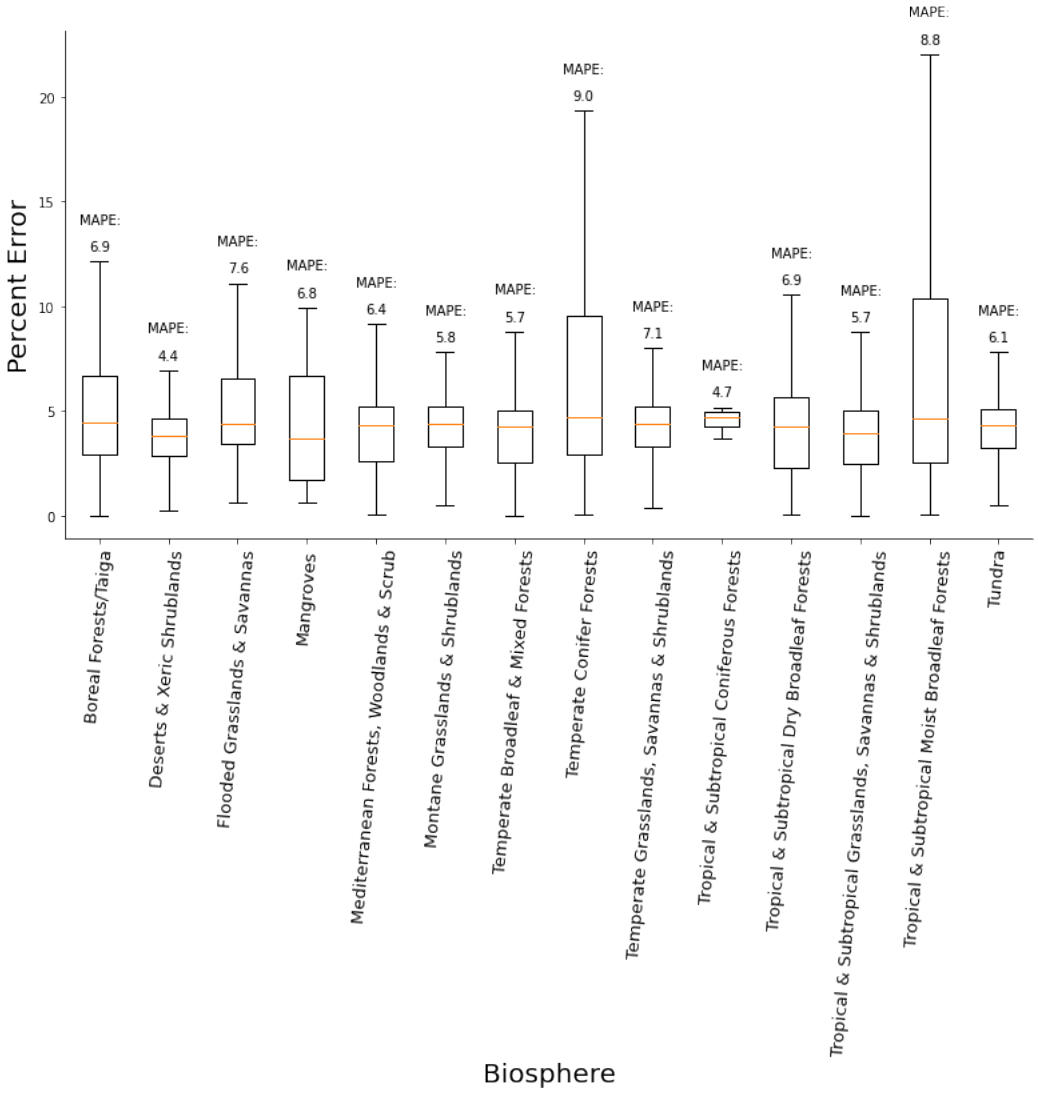

FIGURE 1.7: The error distributions for each biosphere the model was tested on.

they were located in. We then created boxplots (see figure 1.7) to look for patterns in the errors. When looking at Figure 1.7 we see Tropical and Subtropical Moist Broadleaf Forests (TSMF) and Temperate Conifer Forests (TCF) are both skewed to the right with large interquartile ranges and the highest MAPE of all the biospheres (8.97% and 8.83% respectively). A possible reason for the high error in the TSMF is that it is composed of mostly deciduous trees. This could indicate the model does not fully account for seasonal trends. A possible reason for the high error in the TCF is that there were only 314 observations from this biosphere in the testing dataset. Overall, the geographical bias of the model is within an acceptable range. The MAPE for each biosphere is within 4% of each other, indicating the model handles the different biospheres relatively similarly. The model does seem to perform slightly worse on forests with deciduous or mixed type forests.

6 Discussion

Across all continents, we can see that the model was broadly successful in predicting the percent of deforestation that occurred with ranges of accuracy similar to other techniques noted in the literature review. The presented technique does not require region-specific calibration, indicating it may be more suitable to global analyses than other techniques.

This paper opens the possibility for several areas of further research. The first is researching the model's implementation with different types of satellite imagery. Landsat 5 and 8 Top of Atmosphere were used for this project, however there are many other satellites of different spatial and temporal resolution that could provide different benefits. Another extension of this project is to look into global real-time deforestation detection. For this paper, composite images of the year before and the year after the deforestation event is used as input, however a smaller window could be tested.

There are several limitations of this study that can be resolved with further research. This study only looked at one type of CNN, however there is much room for further research into other model architectures. A comparative study can also be done with this CNN and a different preexisting deforestation detection model. For example, BFAST and the U-Net-like CNN mentioned in the

literature review. The comparison of different machine learning and deep learning models on a diverse global dataset can help to isolate the most robust model. A comparison of other CNN architectures could also lead to better results and should be explored as options.

However, even with the best model it is important that deforestation detection modeling goes beyond proof-of-concept research papers and becomes a usable tool. Even if a model has 100% accuracy it has no use if it is not being used. For further study, the development of a user friendly interface for deep learning deforestation breaks detection would be an important tool for the conservation community.

7 Conclusion

The main question driving this research was *To what degree can deforestation be quantified using deep learning techniques?* The purpose of this paper was to extend our ability to track deforestation events. We developed a Convolutional Neural Network that used the before and after image of a deforestation event as inputs. Our results illustrated that deep learning detection of global breaks in forest cover is promising. We achieved a global mean absolute percent error of 7.61%, and less than 10% error on 85% of the data. This compares favorably with previous results of similar studies.

The model created in this research demonstrates two things. First, the model removes the need for region-specific calibration. Our methods required no region-specific calibration yet yielded relatively comparable bias to region-specific models in estimates across the globe. We additionally test the approach of using only two images as inputs for detection. Unlike other approaches that tend to train the model on a stack of images, we trained each before and after image of a deforestation event on separate CNNs. This allows deforestation to be contrasted across various time periods, according to a user's need.

In summary, the CNN presented here illustrates how using satellite imagery from around the world can help to train a robust deforestation detection model. Relying solely on free, publicly available imagery, we were able to develop a method to begin detecting deforestation globally. Extending this approach to

other datasets and platforms could have lasting implications for the future of deforestation detection.

8 Acknowledgements

We would like to thank the committee Dan Runfola (chair), Robert Rose, and Anthony Stefanidis. We acknowledge William Mary Research Computing for providing computational resources and/or technical support that have contributed to the results reported within this paper. We would also like to thank the faculty and students of the William Mary geolab (geolab.wm.edu) for their feedback and support, especially Heather Baier.

Appendix A

Appendix

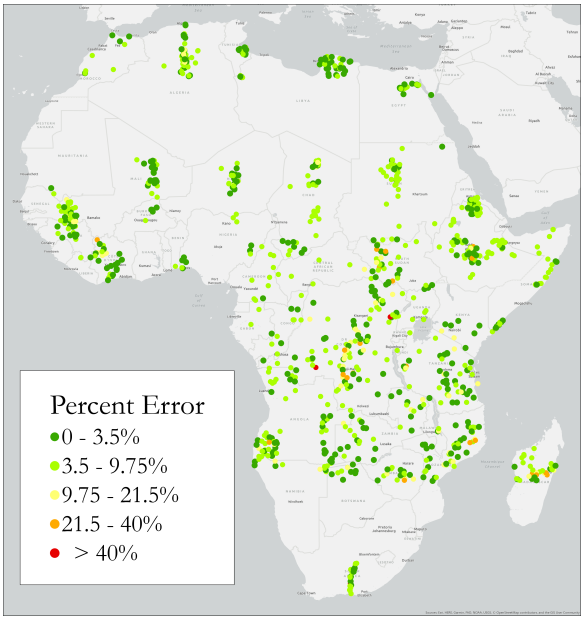

FIGURE A.1: Map of the percent error in Africa

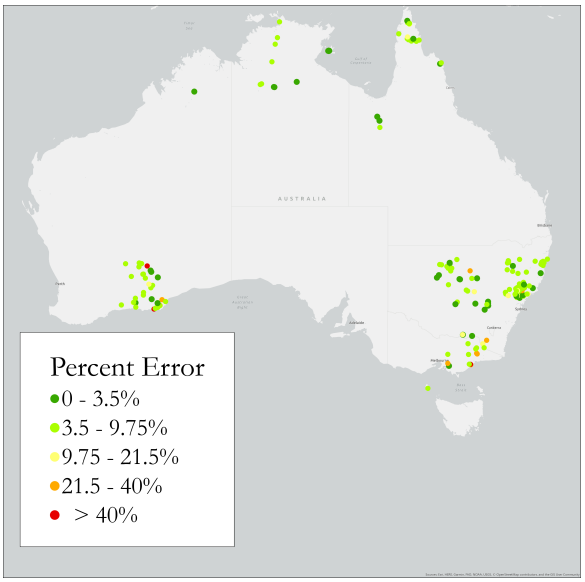

FIGURE A.2: Map of the percent error in Africa

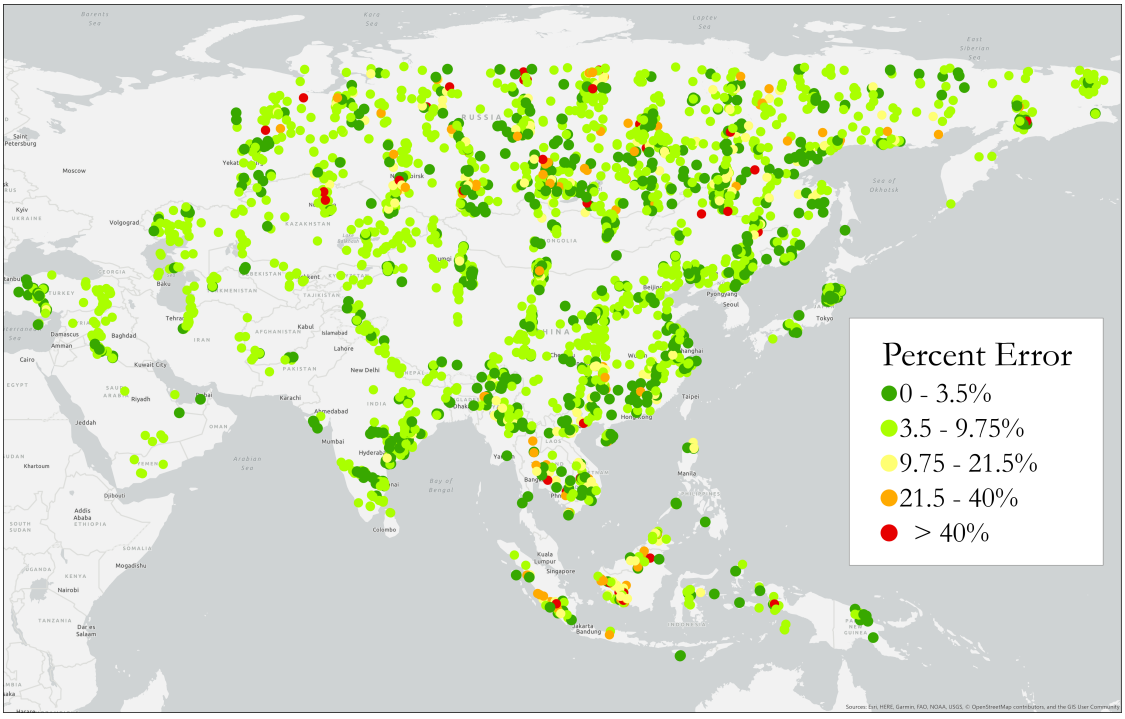

FIGURE A.3: Map of the percent error in Asia

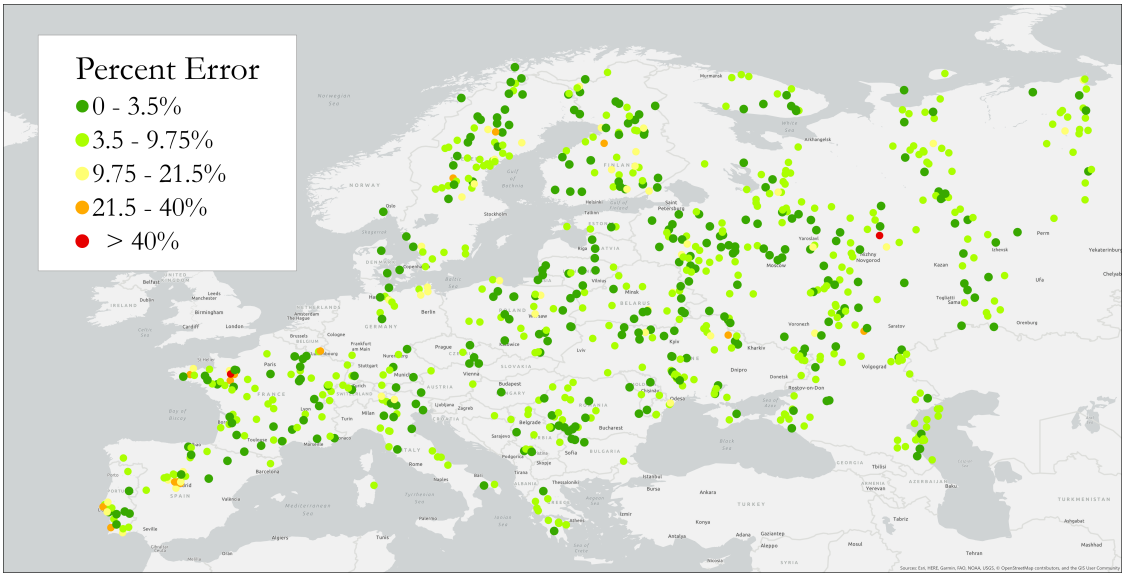

FIGURE A.4: Map of percent error in Europe

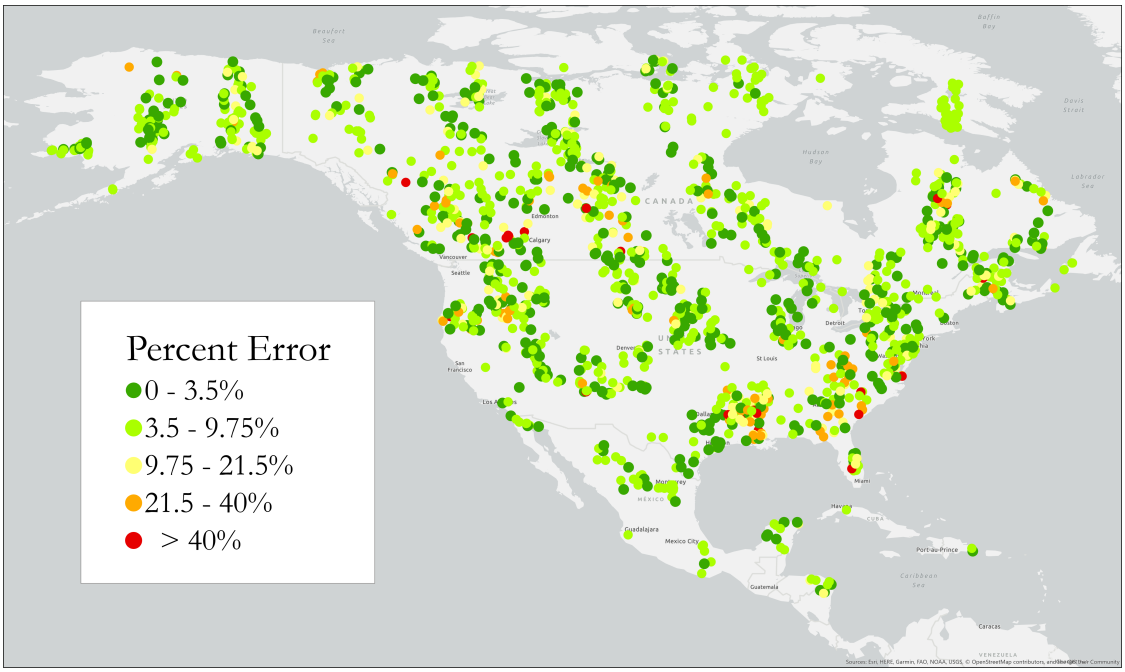

FIGURE A.5: Map of percent error in North America

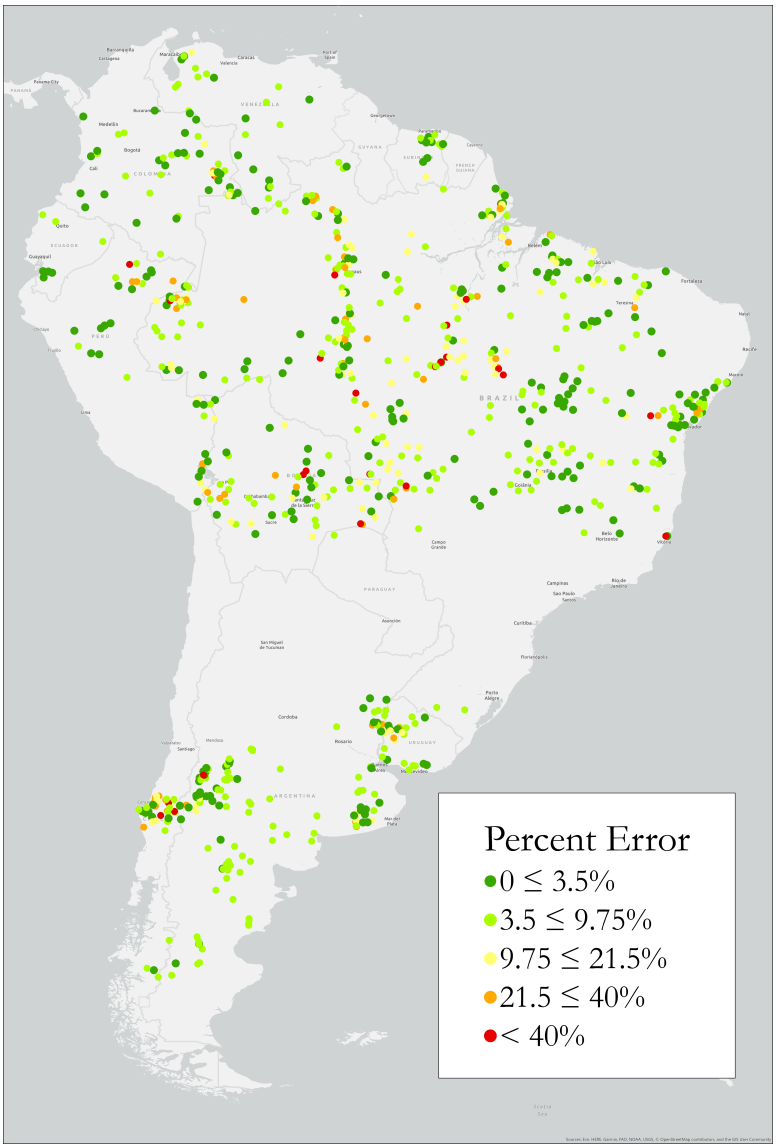

FIGURE A.6: Map of percent error in South America

Bibliography

Acheampong, Emmanuel Opoku et al. (2019). "Deforestation is driven by agricultural expansion in Ghana's forest reserves". In: *Scientific African* 5, e00146. ISSN: 2468-2276. DOI: https://doi.org/10.1016/j.sciaf.2019.e00146. URL: https://www.sciencedirect.com/science/article/pii/S2468227619307070.

Alhindi, Taha J. et al. (2018). "Comparing LBP, HOG and Deep Features for Classification of Histopathology Images". In: *2018 International Joint Conference on Neural Networks (IJCNN)*, pp. 1–7. DOI: 10.1109/IJCNN.2018.8489329.

Amelung, Torsten (1993). "Tropical Deforestation as an International Economic Problem". In: *Economic Progress and Environmental Concerns*. Ed. by Herbert Giersch. Berlin, Heidelberg: Springer Berlin Heidelberg, pp. 233–253. ISBN: 978-3-642-78074-5.

Banskota, Asim et al. (2014). "Forest Monitoring Using Landsat Time Series Data: A Review". In: *Canadian Journal of Remote Sensing* 40.5. Publisher: Taylor & Francis _eprint: https://doi.org/10.1080/07038992.2014.987376, pp. 362–384. DOI: 10.1080/07038992.2014.987376. URL: https://doi.org/10.1080/07038992.2014.987376.

Belward, Alan S. and Jon O. Skøien (2015). "Who launched what, when and why; trends in global land-cover observation capacity from civilian earth observation satellites". In: *ISPRS Journal of Photogrammetry and Remote Sensing* 103, pp. 115–128. ISSN: 0924-2716. DOI: https://doi.org/10.1016/j.isprsjprs.2014.03.009. URL: https://www.sciencedirect.com/science/article/pii/S0924271614000720.

Boafo, James (2013). "The Impact of Deforestation on Forest Livelihoods in Ghana". In: 49, p. 8.

Buhalău, Tudor (2016). "Detecting clear-cut deforestation using Landsat data: A time series analysis of remote sensing data in Covasna County, Romania between 2005 and 2015". In: p. 67.

Chander, Gyanesh, Brian L. Markham, and Julia A. Barsi (2007). "Revised Landsat-5 Thematic Mapper Radiometric Calibration". In: *IEEE Geoscience and Remote Sensing Letters* 4.3, pp. 490–494. DOI: 10.1109/LGRS.2007.898285.

Cramer, Wolfgang, Alberte Bondeau, and Sibyll Schaphoff (Mar. 29, 2004). "Tropical forests and the global carbon cycle: impacts of atmospheric carbon dioxide, climate change and rate of deforestation". In.

D'Almeida, Cassiano et al. (Apr. 1, 2007). "The effects of deforestation on the hydrological cycle in Amazonia: a review on scale and resolution". In: *International Journal of Climatology* 27.5. Publisher: John Wiley & Sons, Ltd, pp. 633–647. ISSN: 0899-8418. DOI: 10.1002/joc.1475. URL: https://doi.org/10.1002/joc.1475 (visited on 04/22/2022).

Dinerstein, Eric et al. (Apr. 2017). "An Ecoregion-Based Approach to Protecting Half the Terrestrial Realm". In: *BioScience* 67.6, pp. 534–545. ISSN: 0006-3568. DOI: 10.1093/biosci/bix014. eprint: https://academic.oup.com/bioscience/article-pdf/67/6/534/17644834/bix014.pdf. URL: https://doi.org/10.1093/biosci/bix014.

Eckert, Sandra et al. (2015). "Trend analysis of MODIS NDVI time series for detecting land degradation and regeneration in Mongolia". In: *Journal of Arid Environments* 113, pp. 16–28. ISSN: 0140-1963. DOI: https://doi.org/10.1016/j.jaridenv.2014.09.001. URL: https://www.sciencedirect.com/science/article/pii/S0140196314001797.

FAO (Sept. 1, 2015). "State of the world's forests: enhancing the socioeconomic benefits from forests". In: *Choice Reviews Online* 53.1, pp. 53–0033–53–0033. ISSN: 0009-4978, 1523-8253. DOI: 10.5860/CHOICE.191454. URL: http://choicereviews.org/review/10.5860/CHOICE.191454 (visited on 04/22/2022).

— (2020). *Global Forest Resources Assessment 2020*. FAO. ISBN: 978-92-5-132974-0. DOI: 10.4060/ca9825en. URL: http://www.fao.org/documents/card/en/c/ca9825en (visited on 04/21/2022).

Finer, Matt et al. (2018). "Combating deforestation: From satellite to intervention". In: *Science* 360.6395. _eprint: https://www.science.org/doi/pdf/10.1126/science.aat1203, pp. 1303–1305. DOI: 10.1126/science.aat1203. URL: https://www.science.org/doi/abs/10.1126/science.aat1203.

Foley, Jonathan A. et al. (2005). "Global Consequences of Land Use". In: *Science* 309.5734. _eprint: https://www.science.org/doi/pdf/10.1126/science.1111772,

pp. 570–574. DOI: 10.1126/science.1111772. URL: https://www.science.org/doi/abs/10.1126/science.1111772.

Galford, Gillian L. et al. (2010). "Greenhouse gas emissions from alternative futures of deforestation and agricultural management in the southern Amazon". In: *Proceedings of the National Academy of Sciences* 107.46. _eprint: https://www.pnas.org/doi
pp. 19649–19654. DOI: 10.1073/pnas.1000780107. URL: https://www.pnas.org/doi/abs/10.1073/pnas.1000780107.

Galiatsatos, Nikolaos et al. (2020). "An Assessment of Global Forest Change Datasets for National Forest Monitoring and Reporting". In: *Remote Sensing* 12.11. ISSN: 2072-4292. DOI: 10.3390/rs12111790. URL: https://www.mdpi.com/2072-4292/12/11/1790.

Gao, Yan et al. (2021). "How BFAST Trend and Seasonal Model Components Affect Disturbance Detection in Tropical Dry Forest and Temperate Forest". In: *Remote Sensing* 13.11. ISSN: 2072-4292. DOI: 10.3390/rs13112033. URL: https://www.mdpi.com/2072-4292/13/11/2033.

Hamunyela, Eliakim et al. (2020). "Implementation of BFASTmonitor Algorithm on Google Earth Engine to Support Large-Area and Sub-Annual Change Monitoring Using Earth Observation Data". In: *Remote Sensing* 12.18. ISSN: 2072-4292. DOI: 10.3390/rs12182953. URL: https://www.mdpi.com/2072-4292/12/18/2953.

Hansen, M. C. et al. (2013). "High-Resolution Global Maps of 21st-Century Forest Cover Change". In: *Science* 342.6160. _eprint: https://www.science.org/doi/pdf/10.1126/scie
pp. 850–853. DOI: 10.1126/science.1244693. URL: https://www.science.org/doi/abs/10.1126/science.1244693.

Hansen, Matthew C., Stephen V. Stehman, and Peter V. Potapov (2010). "Quantification of global gross forest cover loss". In: *Proceedings of the National Academy of Sciences* 107.19. _eprint: https://www.pnas.org/doi/pdf/10.1073/pnas.0912668107, pp. 8650–8655. DOI: 10.1073/pnas.0912668107. URL: https://www.pnas.org/doi/abs/10.1073/pnas.0912668107.

He, Kaiming et al. (2015). "Deep Residual Learning for Image Recognition". In: *CoRR* abs/1512.03385. arXiv: 1512.03385. URL: http://arxiv.org/abs/1512.03385.

Huang, Chengquan et al. (2010). "An automated approach for reconstructing recent forest disturbance history using dense Landsat time series stacks".

In: *Remote Sensing of Environment* 114.1, pp. 183–198. ISSN: 0034-4257. DOI: https://doi.org/10.1016/j.rse.2009.08.017. URL: https://www.sciencedirect.com/science/article/pii/S0034425709002685.

Huete, A. R. (1988). "A soil-adjusted vegetation index (SAVI)". In: *Remote Sensing of Environment* 25.3, pp. 295–309. ISSN: 0034-4257. DOI: https://doi.org/10.1016/0034-4257(88)90106-X. URL: https://www.sciencedirect.com/science/article/pii/003442578890106X.

Jiang, Zhangyan et al. (2008). "Development of a two-band enhanced vegetation index without a blue band". In: *Remote Sensing of Environment* 112.10, pp. 3833–3845. ISSN: 0034-4257. DOI: https://doi.org/10.1016/j.rse.2008.06.006. URL: https://www.sciencedirect.com/science/article/pii/S0034425708001971.

Kattenborn, Teja, Jana Eichel, and Fabian Ewald Fassnacht (Nov. 27, 2019). "Convolutional Neural Networks enable efficient, accurate and fine-grained segmentation of plant species and communities from high-resolution UAV imagery". In: *Scientific Reports* 9.1, p. 17656. ISSN: 2045-2322. DOI: 10.1038/s41598-019-53797-9. URL: https://doi.org/10.1038/s41598-019-53797-9.

Kaufman, Y.J. and D. Tanre (1992). "Atmospherically resistant vegetation index (ARVI) for EOS-MODIS". In: *IEEE Transactions on Geoscience and Remote Sensing* 30.2, pp. 261–270. DOI: 10.1109/36.134076.

Keenan, Rodney J. et al. (2015). "Dynamics of global forest area: Results from the FAO Global Forest Resources Assessment 2015". In: *Forest Ecology and Management* 352, pp. 9–20. ISSN: 0378-1127. DOI: https://doi.org/10.1016/j.foreco.2015.06.014. URL: https://www.sciencedirect.com/science/article/pii/S0378112715003400.

Kislov, Dmitry E. and Kirill A. Korznikov (2020). "Automatic Windthrow Detection Using Very-High-Resolution Satellite Imagery and Deep Learning". In: *Remote Sensing* 12.7. ISSN: 2072-4292. DOI: 10.3390/rs12071145. URL: https://www.mdpi.com/2072-4292/12/7/1145.

Kislov, Dmitry E. et al. (2021). "Extending deep learning approaches for forest disturbance segmentation on very high-resolution satellite images". In: *Remote Sensing in Ecology and Conservation* 7.3. _eprint: https://zslpublications.onlinelibrary.wiley.co

pp. 355–368. DOI: https://doi.org/10.1002/rse2.194. URL: https://zslpublications.onlinelibrary.wiley.com/doi/abs/10.1002/rse2.194.

Klaus Riede (1993). "Monitoring Biodiversity: Analysis of Amazonian Rainforest Sounds". In: *Ambio* 22.8. Publisher: [Springer, Royal Swedish Academy of Sciences], pp. 546–548. ISSN: 00447447, 16547209. URL: http://www.jstor.org/stable/4314145 (visited on 04/22/2022).

Lauer, Donald T (1997). "The Landsat Program: Its Origins, Evolution, and Impacts". In: p. 8.

Lechler, S. et al. (Aug. 2020). "Exploring Nasa's Harmonized Landsat and SENTINEL-2 (hls) Dataset to Monitor Deforestation in the Amazon Rainforest". In: *ISPRS - International Archives of the Photogrammetry, Remote Sensing and Spatial Information Sciences* 43B3, pp. 705–711. DOI: 10.5194/isprs-archives-XLIII-B3-2020-705-2020.

Leitão, Pedro J. et al. (2018). "From sample to pixel: multi-scale remote sensing data for upscaling aboveground carbon data in heterogeneous landscapes". In: *Ecosphere* 9.8. _eprint: https://esajournals.onlinelibrary.wiley.com/doi/pdf/10.1002/ecs2.2298 e02298. DOI: https://doi.org/10.1002/ecs2.2298. URL: https://esajournals.onlinelibrary.wiley.com/doi/abs/10.1002/ecs2.2298.

Lepš, Jan and Věra Hadincová (1992). "How Reliable Are Our Vegetation Analyses?" In: *Journal of Vegetation Science* 3.1. Publisher: Wiley, pp. 119–124. ISSN: 11009233, 16541103. DOI: 10.2307/3236006. URL: http://www.jstor.org/stable/3236006 (visited on 04/22/2022).

Loveland, T. R. et al. (Jan. 1, 2000). "Development of a global land cover characteristics database and IGBP DISCover from 1 km AVHRR data". In: *International Journal of Remote Sensing* 21.6. Publisher: Taylor & Francis, pp. 1303–1330. ISSN: 0143-1161. DOI: 10.1080/014311600210191. URL: https://doi.org/10.1080/014311600210191.

Lunetta, Ross S (1991). "Remote Sensing and Geographic Information System Data Integration:Error Sources and Research Issues". In: *PHOTOGRAMMETRIC ENGINEERING*, p. 11.

MacDicken, Kenneth G. (2015). "Global Forest Resources Assessment 2015: What, why and how?" In: *Forest Ecology and Management* 352, pp. 3–8. ISSN: 0378-1127. DOI: https://doi.org/10.1016/j.foreco.2015.02.006. URL: https://www.sciencedirect.com/science/article/pii/S0378112715000572.

Masolele, Robert N. et al. (2021). "Spatial and temporal deep learning methods for deriving land-use following deforestation: A pan-tropical case study using Landsat time series". In: *Remote Sensing of Environment* 264, p. 112600. ISSN: 0034-4257. DOI: https://doi.org/10.1016/j.rse.2021.112600. URL: https://www.sciencedirect.com/science/article/pii/S0034425721003205.

Mazza, Antonio et al. (2019). "TanDEM-X Forest Mapping Using Convolutional Neural Networks". In: *Remote Sensing* 11.24. ISSN: 2072-4292. DOI: 10.3390/rs11242980. URL: https://www.mdpi.com/2072-4292/11/24/2980.

Minaee, Shervin et al. (2020). "Image Segmentation Using Deep Learning: A Survey". In: *CoRR* abs/2001.05566. arXiv: 2001.05566. URL: https://arxiv.org/abs/2001.05566.

Mitchard, Edward et al. (2015). *Assessment of the accuracy of University of Maryland (Hansen et al.) Forest Loss Data in 2 ICF project areas – component of a project that tested an ICF indicator methodology*. Final Report. The University of Edinburgh.

Mitchell, Anthea L., Ake Rosenqvist, and Brice Mora (Apr. 17, 2017). "Current remote sensing approaches to monitoring forest degradation in support of countries measurement, reporting and verification (MRV) systems for REDD+". In: *Carbon Balance and Management* 12.1, p. 9. ISSN: 1750-0680. DOI: 10.1186/s13021-017-0078-9. URL: https://doi.org/10.1186/s13021-017-0078-9.

Miura, Satoru et al. (2015). "Protective functions and ecosystem services of global forests in the past quarter-century". In: *Forest Ecology and Management* 352, pp. 35–46. ISSN: 0378-1127. DOI: https://doi.org/10.1016/j.foreco.2015.03.039. URL: https://www.sciencedirect.com/science/article/pii/S0378112715001784.

Nath, Biswajit and Shukla Acharjee (2013). "Forest Cover Change Detection using Normalized Difference Vegetation Index (NDVI) : A Study of Reingkhyongkine Lake's Adjoining Areas, Rangamati, Bangladesh". In: p. 7.

Othman, M A et al. (2018). "Tropical deforestation monitoring using NDVI from MODIS satellite: a case study in Pahang, Malaysia". In: *IOP Conference Series: Earth and Environmental Science* 169, p. 012047. DOI: 10.1088/1755-1315/169/1/012047. URL: https://doi.org/10.1088/1755-1315/169/1/012047.

Ozturk, Ozan, Batuhan Saritürk, and Dursun Zafer Seker (Dec. 6, 2020). "Comparison of Fully Convolutional Networks (FCN) and U-Net for Road Segmentation from High Resolution Imageries". In: *International Journal of Environment and Geoinformatics* 7.3. Number: 3, pp. 272–279. DOI: 10.30897/ijegeo.737993. URL: https://dergipark.org.tr/en/pub/ijegeo/issue/56780/737993 (visited on 04/22/2022).

Romijn, Erika et al. (2015). "Assessing change in national forest monitoring capacities of 99 tropical countries". In: *Forest Ecology and Management* 352, pp. 109–123. ISSN: 0378-1127. DOI: https://doi.org/10.1016/j.foreco.2015.06.003. URL: https://www.sciencedirect.com/science/article/pii/S0378112715003291.

Roy, D. P. et al. (2014). "Landsat-8: Science and product vision for terrestrial global change research". In: *Remote Sensing of Environment* 145, pp. 154–172. ISSN: 0034-4257. DOI: https://doi.org/10.1016/j.rse.2014.02.001. URL: https://www.sciencedirect.com/science/article/pii/S003442571400042X.

Schroeder, Todd A. et al. (2011). "Mapping wildfire and clearcut harvest disturbances in boreal forests with Landsat time series data". In: *Remote Sensing of Environment* 115, pp. 1421–1433.

Schultz, Michael et al. (2018). "Forest Cover and Vegetation Degradation Detection in the Kavango Zambezi Transfrontier Conservation Area Using BFAST Monitor". In: *Remote Sensing* 10.11. ISSN: 2072-4292. DOI: 10.3390/rs10111850. URL: https://www.mdpi.com/2072-4292/10/11/1850.

Sefrin, Oliver, Felix M. Riese, and Sina Keller (2021). "Deep Learning for Land Cover Change Detection". In: *Remote Sensing* 13.1. ISSN: 2072-4292. DOI: 10.3390/rs13010078. URL: https://www.mdpi.com/2072-4292/13/1/78.

Shahedi, Maysam et al. (2020). "A Study on U-Net Limitations in Object Localization and Image Segmentation".

Shyamsundar, Priya et al. (2021). "Global forces of change: Implications for forest-poverty dynamics". In: *Forest Policy and Economics* 133, p. 102607. ISSN: 1389-9341. DOI: https://doi.org/10.1016/j.forpol.2021.102607. URL: https://www.sciencedirect.com/science/article/pii/S1389934121002136.

Sylvain, Jean-Daniel, Guillaume Drolet, and Nicolas Brown (2019). "Mapping dead forest cover using a deep convolutional neural network and digital

aerial photography". In: *ISPRS Journal of Photogrammetry and Remote Sensing* 156, pp. 14–26. ISSN: 0924-2716. DOI: https://doi.org/10.1016/j.isprsjprs.2019.07.010. URL: https://www.sciencedirect.com/science/article/pii/S0924271619301777.

Torres, Daliana Lobo et al. (2021). "Deforestation Detection with Fully Convolutional Networks in the Amazon Forest from Landsat-8 and Sentinel-2 Images". In: *Remote Sensing* 13.24. ISSN: 2072-4292. DOI: 10.3390/rs13245084. URL: https://www.mdpi.com/2072-4292/13/24/5084.

UN-REDD (2014). *Guidance on Conducting REDD+ Corruption Risk Assessments (REDD+ CRA)*. UN-REDD.

USGS (Jan. 1, 2018). *Landsat Collections*. Report 2018-3049. Reston, VA, p. 2. DOI: 10.3133/fs20183049. URL: http://pubs.er.usgs.gov/publication/fs20183049.

Verbesselt, Jan, Achim Zeileis, and Martin Herold (2012). "Near real-time disturbance detection using satellite image time series". In: *Remote Sensing of Environment* 123, pp. 98–108. ISSN: 0034-4257. DOI: https://doi.org/10.1016/j.rse.2012.02.022. URL: https://www.sciencedirect.com/science/article/pii/S0034425712001150.

Verbesselt, Jan et al. (2010a). "Detecting trend and seasonal changes in satellite image time series". In: *Remote Sensing of Environment* 114.1, pp. 106–115. ISSN: 0034-4257. DOI: https://doi.org/10.1016/j.rse.2009.08.014. URL: https://www.sciencedirect.com/science/article/pii/S003442570900265X.

Verbesselt, Jan et al. (2010b). "Phenological change detection while accounting for abrupt and gradual trends in satellite image time series". In: *Remote Sensing of Environment* 114.12, pp. 2970–2980. ISSN: 0034-4257. DOI: https://doi.org/10.1016/j.rse.2010.08.003. URL: https://www.sciencedirect.com/science/article/pii/S0034425710002336.

Viera, ICG et al. (2008). "Deforestation and threats to the biodiversity of Amazonia". In: *Brazilian Journal of Biology* 68.4.

Waring, R.H. and S. W. Running (1998). *Forest Ecosystems: Analysis at Multiple Scales*. New York: Academic Press.

Woodcock, C. E. et al. (May 2008). *Free Access to Landsat Imagery*.

Zon, R. and W.N. Sparhawk (1923). *Forest resources of the world*. Vol. 2. McGraw-Hill Book Company, Incorporated.